Preparation, Characterization, and Exfoliation of Graphite Perfluorooctanesulfonate

Zhengwei Zhang and Michael M. Lerner*

Department of Chemistry and Center for Advanced Materials Research, Oregon State University, Corvallis, Oregon 97331-4003

Received August 2, 1995. Revised Manuscript Received September 18, 1995[⊗]

Air-stable graphite compounds with perfluorooctanesulfonate, $C_xC_8F_{17}SO_3$, are prepared by electrochemical oxidation of HOPG chips or SP-1 graphite powder in $LiC_8F_{17}SO_3$ (saturated)/CH_3NO_2 electrolyte. XRD patterns of several single-stage products indicate that highly ordered intercalation compounds form with $d_i = 24.6-24.9$ Å for stages (n) = 3−7 or 26.6 Å for $n = 2$, supporting the model of a bilayer of perfluoroalkylsulfonate anions within the intercalated galleries. Gravimetric and thermogravimetric data provide x for $n = 2-6$. Consistent with the bilayer model, the C/anion ratio is found to be much lower than in small-anion intercalation compounds. Ambient temperature exfoliation occurs when a high-stage graphite sulfate is anodized in the $C_8F_{17}SO_3^-$-containing electrolyte.

Introduction

The anodization of graphite to form intercalation compounds has been known in both concentrated acids[1,2] and organic electrolytes for several decades.[3−7] A variety of anion types have been incorporated by the electrochemical route, including primarily oxoanions (e.g., SO_4^{2-} or HSO_4^{2-}, ClO_4^-, and NO_3^-) and fluoroanions (e.g., F^-, HF_2^-, BF_4^-, and PF_6^-).[8−10] The incorporation of anions is accompanied by the reversible uptake of coordinating neutral molecules, as indicated in the following reaction formulations:

$$C_x \xrightarrow[PC]{-e^-,\ LiPF_6} C_xPF_6{\cdot}nPC \qquad \text{[refs 4−6]} \qquad (1)$$

$$C_x \xrightarrow[\text{anhydrous HF}]{-e^-,\ NaHF_2} C_xHF_2{\cdot}nHF \qquad \text{[refs 9, 10]} \qquad (2)$$

(PC = propylene carbonate). The various combinations of anions and co-intercalating neutral species provide a large number of intercalation reactions for study, and by the electrochemical method alone several dozen different systems have been explored. Additionally, some complexity is introduced by systems (examples include sulfate/bisulfate and fluoride/bifluoride) where multiple anionic species are possible. Taken together with the larger number of reports on chemical oxidation of graphite, acceptor-type intercalation compounds constitute a large and widely studied family.

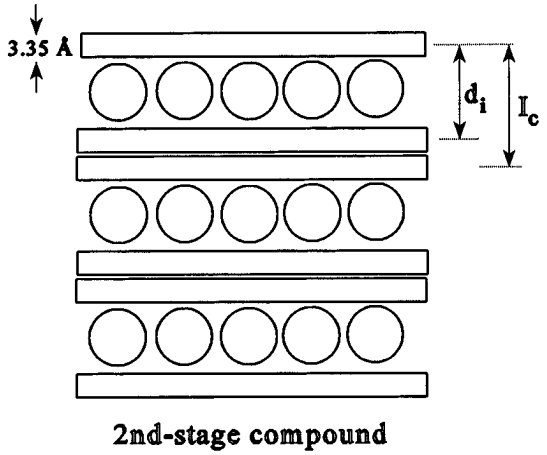

Figure 1. Relation of distance parameters, d_i and I_c associated with intercalation compounds. A second-stage compound is pictured.

Despite the breadth of the chemistry indicated above, it is notable that the anionic intercalants are almost always small, hard (low polarizability), and of high symmetry. The "height" of the intercalated carbon gallery (d_i in Figure 1) relates to the packing of these anions and coordinating solvent between the carbon sheets, so that d_i is usually close to 8 Å for the fluoroanion and oxoanions compounds. The largest values for d_i, associated with chlorometallates of Fe, Al, and other metals, are approximately 10 Å.[8]

After a long history of work in the area, the intergallery structures and host−guest chemistry observed for graphite compounds are not nearly as varied as those with other layered hosts. Expansions in layered metal disulfides, metal oxides, and clays can be 20−30 Å or more,[11−13] and the complete exfoliation of layered hosts

[⊗] Abstract published in *Advance ACS Abstracts,* November 1, 1995.

(1) Rudorff, W.; Hoffmann, U. *Z. Anorg. Allg. Chem.* **1938**, 238.
(2) Bottomley, M. J.; Parry, G. S.; Ubbelohde, A. R.; Young, D. A. *J. Chem. Soc.* **1963**, 5675.
(3) Dunning, J.; Tiedemann, W.; Hsueh, L.; Bennion, D. *J. Electrochem. Soc.* **1971**, *118*, 1886.
(4) Besenhard, J.; Fritz, H. P. *J. Electrochem. Soc.* **1972**, *119*, 1697.
(5) Jobert, A.; Touzain, P.; Bonnetain, L. *Carbon* **1981**, *19*, 193.
(6) Billaud, D.; Chenite, A.; Metrot, A. *Carbon* **1982**, *20*, 493.
(7) Marcus, B.; Touzain, P. *J. Solid State Chem.* **1988**, *77*, 223.
(8) Bartlett, N.; McQuillan, B. W. In *Intercalation Chemistry*; Whittingham, S. M., Jacobsen, A. J., Eds.; Academic Press: New York, 1982.
(9) Watanabe, N.; Touhara, H.; Nakajima, T.; Bartlett, N.; Mallouk T.; Selig, H. In *Inorganic Solid Fluorides*; Hagenmuller, P., Ed.; Academic Press: New York, 1985.
(10) Hagiwara, R.; Bartlett, N. In *Fluorine-Carbon and Fluoride Carbon Materials*; Nakajima, T., Ed.; Marcel Dekker: New York, 1995.
(11) Pinnavaia, T. *Science* **1983**, *220*, 365.
(12) Cavani, F.; Trifiro, F.; Vaccari, A. *Catal. Today* **1992**, *11*, 173.
(13) For example, a series of alkylammonium ions within layered $TiNbO_5^-$ layers in: Rebbah, H.; Borel, M.; Raveau, B. *Mater. Res. Bull.* **1980**, *15*, 317.

0897-4756/96/2808-0257$12.00/0

into single-sheet colloids are well-known for some layered oxides (for example, the smectite clays or MoO_3) and metal disulfides.[14,15] Nanocomposition, complex intercalant structures, ion and solvent-exchange, and catalytic properties have been studied for many of these layered hosts.[11−17] The reason for the relatively limited extent of the chemistry of oxidized carbon layers is certainly the high potential associated with graphite oxidation. Only the most oxidatively robust species remain stable at these potentials, and water (except in highly concentrated acids), air, and most organic solvents must be excluded.

In 1986, Ruisinger and Boehm extended earlier work on the formation of graphite trifluoromethanesulfonates[18] with the investigation of graphite intercalation by perfluorobutanesulfonate, $C_4F_9SO_3^-$.[19] Graphite compounds were prepared by anodization of graphite in the anhydrous acid $C_4F_9SO_3H$ or in a PC/acid solution. On the basis of diffraction data which indicated very large values for d_i (>20 Å), a structural model was proposed with bilayers of $C_4F_9SO_3^-$ arranged with nonpolar ends oriented into the gallery centers. These bilayer structures are commonly observed when surfactants are intercalated to form "organoclays"[11,12] and with other layered hosts[13] but had not been previously seen in graphite compounds. In addition, the expansions reported greatly exceed those known for other graphite compounds. The same research group subsequently communicated that related structures can develop from intercalation of a series of sulfonates ($C_nH_{2n+1}SO_3$, n = 1−5) and perfluorosulfonates ($C_nF_{2n+1}SO_3$, n = 4, 6, 8).[20] The larger anions are also reported to form bilayer intercalation structures, with d_i = 34.21(50) Å noted for second-stage $C_xC_8F_{17}SO_3$.

In this paper, we report fully on our previous descriptions of the structural details for the $C_xC_8F_{17}SO_3$ compounds obtained by anodization of graphite in an organic electrolyte.[21] Some double-ion reactions are investigated, and we describe conditions where some of these graphite compounds delaminate at ambient temperature.

Experimental Section

Nitromethane (Aldrich, 99%) and H_2SO_4 (Aldrich, 98%) were used as received. $LiC_8F_{17}SO_3$ (3M, experimental product) was treated with 1 atm of F_2 at ambient temperature for 24 h to destroy traces of oxidizable impurities and then evacuated for 24 h. Although the color of the salt changed from light brown to white following fluorine treatment, the XRD patterns remained unchanged and did not indicate any crystalline impurities. In all reactions, the purified salt was added in excess to form a saturated electrolyte solution.

Electrochemical analyses and syntheses were performed at ambient temperature in a two-compartment, sealed glass cell which has been described previously.[22] Two types of graphite were used in working electrodes: (1) HOPG, Atomgraph Co., 0.63° mosaic and (2) SP-1 powder, Union Carbide, 100 μm average particle diameter. HOPG electrodes were fabricated by folding a chip (approximately 0.3 × 0.5 × 0.2−1.0 mm) into a square of Pt mesh welded to a Pt lead. For the graphite powder, 5−10% inert binder (EPDM, Exxon) was dissolved in cyclohexane and stirred with the graphite. The resulting slurry was painted onto a Pt mesh electrode (geometric surface ≈ 1 cm^2) and dried.

Galvanostatic oxidation was carried out by applying a current density between 1 and 4 mA/g carbon, resulting in the formation of the graphite compound via

$$C_x \xrightarrow[CH_3NO_2]{-e^-,\ LiSO_3C_8F_{17}} C_xSO_3C_8F_{17}\cdot yCH_3NO_2 \qquad (3)$$

Volatile species were subsequently removed from products by evacuation for 12 h at ambient temperature. All product analyses were performed on these evacuated materials.

$$C_xSO_3C_8F_{17}\cdot yCH_3NO_2 \xrightarrow{evac} C_xSO_3C_8F_{17} \qquad (4)$$

The dried products obtained were found to be very stable to ambient conditions. Diffraction patterns were unchanged after exposure of the sample to air for several weeks. Mass and thickness changes were determined on the dried products obtained from HOPG electrodes.

In some experiments, graphite sulfate or perchlorate was formed by galvanostatic oxidation at 10 mA/g of C in concentrated sulfuric or perchloric acids. The product was rinsed with acetone briefly (approximately 3 s) to remove excess solvent, and dried in vacuo for 15 min. The graphite sulfate or perchlorate was then further anodized in the $LiC_8F_{17}SO_3$(saturated)/CH_3NO_2 electrolyte until no changes were observed in a potential/charge plot.

X-ray powder diffraction (XRD) data were collected at ambient temperature on a Siemens D5000 powder diffractometer ($2° < 2\theta < 60°$) at 0.02°/s using Cu Kα radiation (1.5418 Å). HOPG samples were mounted directly on a sample holder and cleaved to expose fresh surfaces and test for product homogeniety. Pressed pellets of the reaction products using SP1 powder was employed. TGA data were obtained using a Netzsch, Inc. STA 419 C thermal analyzer. Samples were loaded into aluminum pans; the sample chamber was evacuated and back-filled with He. Thermal scans from ambient to 400 °C were performed at 10 °C/min. An AMRAY 1000A scanning electron microscope was employed for microscopic imaging.

Results and Discussion

The intercalation reaction rate is limited by ion diffusion into the graphite galleries, and this diffusion rate is determined by ion size and charge. The current observed in slow cyclic voltammetry (Figure 2) with the large perfluorosulfonate anions is dampened relative to that corresponding to intercalation of trifluoromethanesulfonate ($CF_3SO_3^-$), and a long current tail on the reverse scan indicates a cathodic reaction (deintercalation) back to the endpoint (+0.5 V). These changes in voltammogram shape are consistent with the slower kinetics for intercalation and deintercalation expected for the larger anions. A comparison of pulsed charge experiments for graphite oxidation of $CF_3SO_3^-$ and $C_8F_{17}SO_3^-$ (Figure 3) evinces a similar conclusion; in this case a much greater overpotential is associated with the incorporation of the larger anions. The oxidation overpotential is approximately equal to the potential difference between charging and resting modes, i.e., the

(14) Murphy, D.; Hull, G. *J. Chem. Phys.* **1975**, *62*, 973.
(15) Yang, D.; Sandoval, S.; Divigalpitiya, M.; Irwin, J.; Frindt, R. *Phys. Rev. B* **1991**, *43*, 12053.
(16) Lemmon, J.; Wu, J.; Lerner, M. In *Hybrid Organic/Inorganic Composites*; Mark, J., Lee, C., Bianconi, P., Eds.; ACS Symp. Series 585; ACS: Washington DC, 1995; Chapter 5.
(17) Ruiz-Hitsky, E. *Adv. Mater.* **1993**, *5*, 334.
(18) Horn, D.; Boehm, H. *Mater. Sci. Eng.* **1977**, *31*, 87.
(19) (a) Ruisinger, B.; Boehm, H. *Angew. Chem., Int. Ed. Engl.* **1987**, *26*, 253. (b) Ruisinger, B.; Boehm, H. *Carbon* **1993**, *31*, 1131.
(20) Boehm, H.; Helle, W.; Ruisinger, B. *Synth. Met.* **1988**, *23*, 395.
(21) (a) Zhang, Z.; Lerner, M. MRS National Meeting, San Francisco, April, 1994. (b) Zhang, Z.; Lerner, M. Electrochem. *Soc. Natl. Mtg.*, San Francisco, May, 1994.
(22) Zhang, Z.; Lerner, M. *J. Electrochem. Soc.* **1993**, *140*, 742.

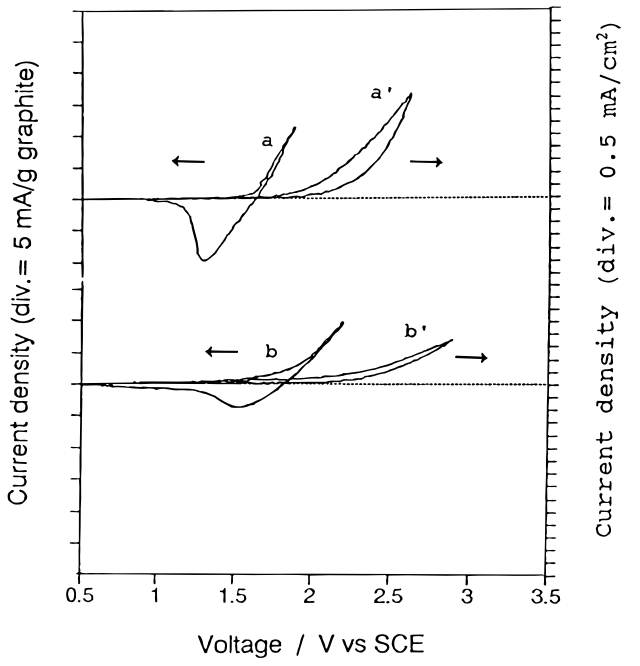

Figure 2. Slow cyclic voltammetry for graphite in (a) $LiCF_3SO_3/CH_3NO_2$ and (b) $LiC_8F_{17}SO_3$(saturated)/CH_3NO_2. The voltammograms labeled a′ and b′ test the electrolyte stabilities against a Pt electrode.

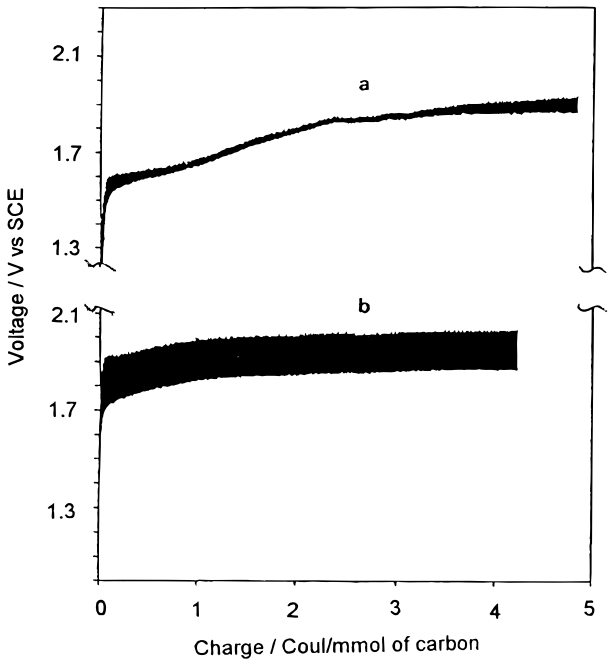

Figure 3. Pulsed galvanostatic charge curves (t_{on} = 60 s, t_{off} = 60 s) for graphite in (a) $LiCF_3SO_3/CH_3NO_2$ and (b) $LiC_8F_{17}SO_3$(saturated)/CH_3NO_2.

potential width of the traces displayed. The overpotential increases from approximately 25 mV for triflate to >200 mV for the larger anion.

Two effects arising from the slower reaction kinetics and associated larger overpotentials are significant in these experiments. First, although CH_3NO_2 was chosen as a solvent in these syntheses due to its high oxidative stability, the overall charging efficiency (calculated as charge on graphite/charge applied) is relatively low. The intercalation of small anions in nitromethane can proceed with efficiencies greater than 0.95,[6,22] whereas efficiencies for these reactions are estimated at 0.2–0.7, depending on charging rate, from observed mass changes using HOPG electrodes and the $LiC_8F_{17}SO_3$ (saturated)/CH_3NO_2 electrolyte. As other CH_3NO_2-based electrolytes have been observed to slowly oxidize near the potential applied in these electrosyntheses,[22] solvent degradation is presumed to be the principal side reaction. The total current applied to the cells is small (typically 2 C/15 mL of electrolyte), which ensures that a very small fraction of the solvent decomposes. At higher charging rates the HOPG electrodes become passivated with an insulating surface; syntheses must therefore be carried out slowly. The low charge rates and efficiencies combine to require long reaction times, often greater than 1 week, to obtain highly intercalated (low-stage) products. XRD analyses at several different locations in all the HOPG products confirm an advantage of the slower reactions—that even HOPG electrodes produce homogeneous products at these charge rates.

Table 1. Diffraction, Expansion, and Gravimetric Data Obtained on Products of the Electrooxidation of Graphite in $LiC_8F_{17}SO_3$(saturated)/CH_3NO_2[a]

			t/t_0			
I_c/Å	stage	d_i/Å	obs	calc	m/m_0	x in $C_xSO_3C_8F_{17}$
44.7	7	24.6				
41.3	6	24.6	1.9	2.1	1.5	83
38.1	5	24.7			1.8	52
34.9	4	24.9	2.5	2.6	2.4	30
31.8	3	25.1	3.2	3.1	2.5	28
29.9(s)	2	26.6		5.0	3.5	17
31.6(m)	3	24.9				

[a] The final masses reported are those recorded after evacuation for 12 h.

A second effect of the high overpotentials in these electrosyntheses relates to the transitions in the galvanostatic charging curve that arise from stage changes. These features are characteristic of the quasi-equilibrium curves obtained with small ions[23] and provide an in situ indication of the stage of the graphite compound during anodization. In the reactions with these large anions, however, the staging transitions are masked by the large overpotentials, which bring the electrode potential close to the electrolyte decomposition potential, and the stage of the product is not apparent during the reaction.

For the reasons described above, the stage of the product cannot be reliably deduced from either the amount of charge applied or features present in the charge curve itself. Most experiments therefore lead to mixed-stage products. By repeated trials and an empirical correlation of applied charge with mass uptake and XRD data, several single-stage and nearly single-stage products have been successfully obtained (Table 1). A first-stage compound has not been prepared, however, due to delamination of the graphite anodes.

The products obtained are well-ordered along the stacking directions and typically exhibit 10–20 (00*l*) reflections. Representative diffraction patterns of a single-stage (Figure 4a) and a mixed-stage product (4b) are shown, and these patterns are indexed in Table 2. These compounds are prepared in separate experiments, and the sets of reflections indexed to a third-stage compound show small variations in intensity and position.

(23) Metrot, A. *Synth. Met.* **1983**, *7*, 177.

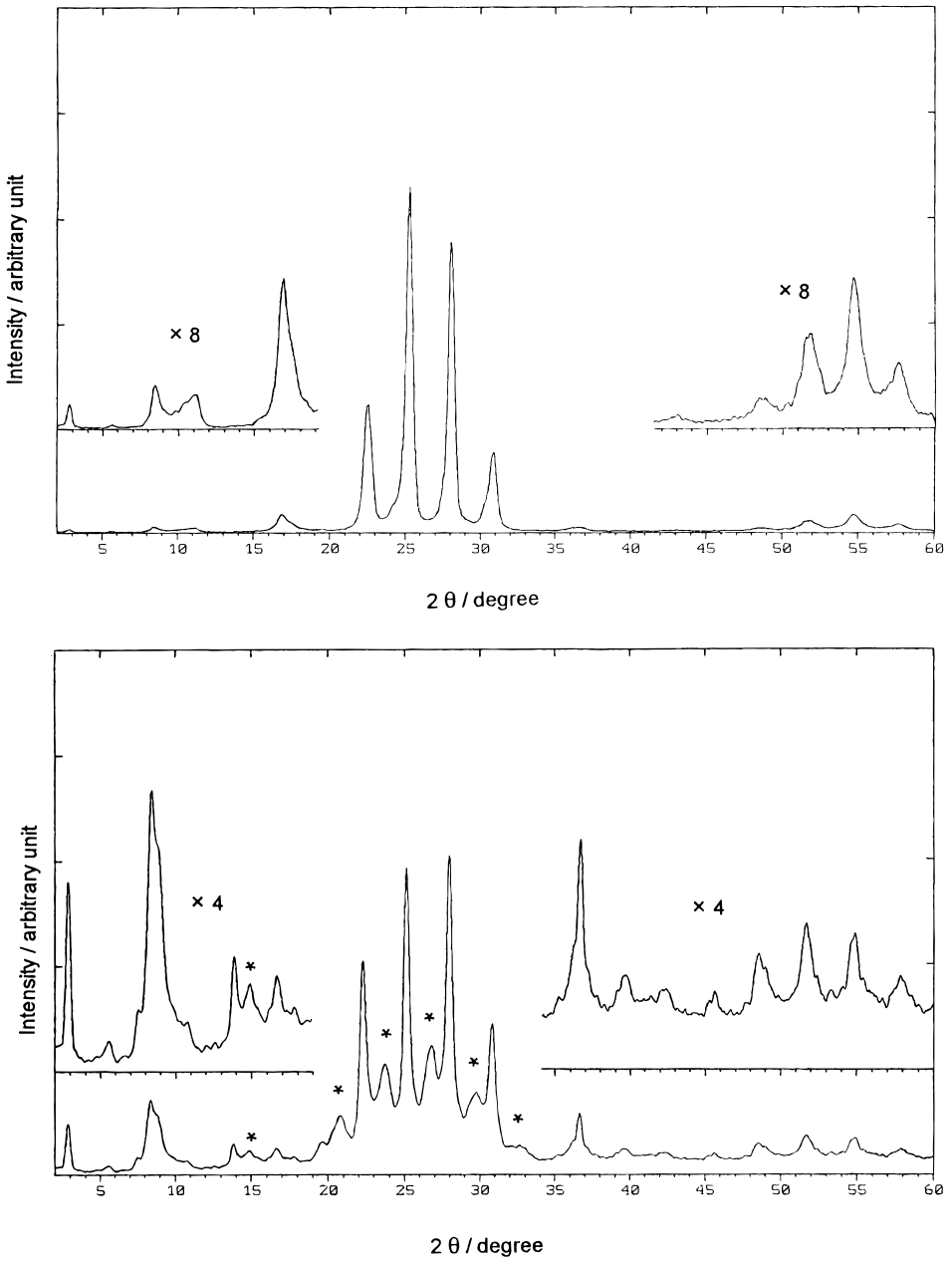

Figure 4. X-ray diffraction patterns (using Cu Kα = 1.5418 Å radiation) for (a, top) a single-phase product containing a third-stage compound, I_c = 31.77(11) Å, and (b, bottom) a product containing a mixture of third-stage, I_c = 31.78(10) Å, and second-stage, I_c = 29.99(8) Å compounds. Starred peaks in (b) arise from the third-stage compound.

Since these are new graphite compounds, with much different (larger) values for d_i than compounds with small, harder anions such as $CF_3SO_3^-$ or SO_4^{2-}, the relation between the experimentally determined *c*-repeat distance (I_c) provided in Table 2 and d_i is not apparent for any single product. The equation

$$d_i = I_c - (n - 1)3.354 \text{ Å} \qquad (5)$$

where n = stage, cannot be used to determine d_i unless both I_c and the product stage are known. In this study, I_c is measured directly by experiment and the stage is determined from comparison of several different patterns of single-phase products, where a solution is sought that provides a relatively constant value of d_i for the different stages. The independence of d_i and stage, as has been generally observed in other graphite compounds, is expected if the gallery occupancy is the same for all stages. The I_c, stage assignments, and calculated d_i values are averaged for single-stage and nearly single-stage products and displayed in Table 1. The value of d_i is nearly constant at 24.6−24.9 for n = 3−7 but is larger for n = 2 (26.6 Å).

An increase in d_i for first-stage compounds of ≈0.2−0.5 Å has been noted in other graphite compounds, although the difference observed here is significantly larger and arises where n = 2. During the intercalation of anionic bilayers, it is the second-stage compound that first contains an anionic layer associated with all carbon sheets, and it may be the repulsion of positive charges on these carbon sheets that causes an increase in the repeat distance along *c*. Alternatively, the increase in d_i for the second-stage compound might indicate an increase in the angle of inclination or a decrease in nestling of anion layers.

The stage assignments can be further substantiated by relating the macroscopic observation of ratio of

Table 2. Indexing of Diffraction Patterns in Figures 4

a

rel *I*	*d*(obs)/Å	*d*(calc)/Å	index
0.9	31.79	31.77	(001)
1.5	10.42	10.59	(003)
1.2	7.976	7.942	(004)
5.4	5.249	5.295	(006)
36	3.945	3.971	(008)
100	3.520	2.530	(009)
92	3.175	3.177	(0010)
25	2.896	2.888	(0011)
1.3	2.454	2.443	(0013)
1.0	1.873	1.869	(0017)
3.1	1.763	1.765	(0018)
5.1	1.676	1.672	(0019)
2.2	1.598	1.589	(0020)

b

			index	
rel *I*	*d*(obs)/Å	*d*(calc)/Å	3rd stage	2nd stage
17	31.02	31.78	(001)	
3	15.82	15.89	(002)	
23	10.59	10.59	(003)	
11	6.400	6.356	(005)	
8	5.937	6.000		(005)
8	5.326	5.297	(006)	
11	4.521	4.540	(007)	
18	4.277	4.284		(007)
66	3.989	3.973	(008)	
33	3.743	3.749		(008)
95	3.541	3.531	(009)	
39	3.325	3.332		(009)
100	3.186	3.178	(0010)	
24	2.988	2.999		(0010)
45	2.896	2.889	(0011)	
9	2.738	2.726		(0011)
19	2.450	2.444	(0013)	
8	2.263	2.270	(0014)	
7	2.148	2.142		(0014)
7	1.985	1.986, 1.999	(0016)	(0015)
9	1.872	1.869, 1.874	(0017)	(0016)
12	1.765	1.766, 1.764	(0018)	(0017)
11	1.668	1.672, 1.666	(0019)	(0018)
8	1.594	1.589, 1.578	(0020)	(0019)

HOPG sample thickness after anodization to that of the starting sample, t/t_0, to the ratio that may be calculated from changes in the microscopic structure where both d_i and n are known:

$$\frac{t}{t_0} = \frac{d_i + (n-1)(3.35\ \text{Å})}{n(3.35\ \text{Å})} \qquad (6)$$

Observed and calculated values for t/t_0 are listed in Table 1. The HOPG samples swell dramatically at high charging and begin to delaminate when a second-stage compound is formed. Powder samples also swell and fall off the Pt mesh when oxidized beyond the second stage. These observations are not unreasonable when considering the dramatic change in electrode volumes associated with low-stage compounds: an 8-fold volume expansion (all along *c*) is calculated for the first stage compound relative to graphite.

In molecular modeling of the bilayer structure,[24] an inclination angle of the fluorocarbon chain relative to the graphite sheets of approximately 60° is employed to allow the oxygens in the $-SO_3$ unit to lie flat on the carbon sheet surface. All all-trans conformation for the carbon chains is also employed as the lowest energy state for the perfluorinated anions. When anions are allowed to nestle by 2−3 Å where the perfluorocarbon chains meet at the gallery centers (Figure 5), a value of $d_i \approx 24-25$ Å is obtained, in good agreement with the experimentally derived values for higher stage compounds. The stoichiometries obtained experimentally indicate that the anions are not closely packed within the intercalated galleries, which should allow for the significant nestling of anions suggested in Figure 5. The generation of very large galleries in these compounds therefore agrees qualitatively with Boehm and coworkers reports, although the gallery heights found in this study are considerably less than that obtained previously ($d_i = 34.21$) for preparation of the second-stage compound directly from the acid.[18] Some differences in gallery heights and packing densities may be expected from the different electrolytes and conditions employed, but the large difference in these values suggests that the initial studies may have incorrectly assigned the product stages.

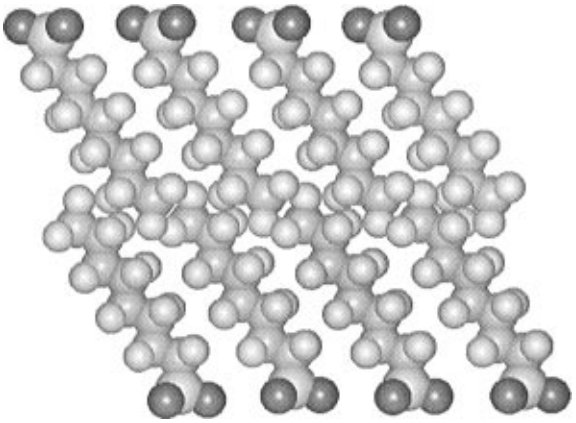

Figure 5. Molecular model for the intercalant structure in $C_xC_8F_{17}SO_3$. The inclination angle is set at 60°, and anions nestle by 2−3 Å at the gallery center.

The extent of incorporation of nitromethane within the galleries during anodization was not directly evaluated, but the evacuated products contain very little of the solvent. Mass losses in TGA below 120 °C (bp of CH_3NO_2 = 101 °C) on the evacuated products are less than 1%.

The stoichiometries for products obtained are therefore formulated as $C_xC_8F_{17}SO_3$, and values are calculated for *x* from gravimetric analyses according to

$$x = \frac{\text{mw}(C_8F_{17}SO_3^-)}{12.0\ \text{g/mol} \times (1 - m/m_0)} = \frac{41.6}{1 - m/m_0} \qquad (7)$$

and provided in Table 1. The anion content is clearly much larger than that for other graphite compounds. For comparison, the approximate values of *x* for a second-stage graphite compounds prepared by electrochemical oxidation in H_2SO_4, $HClO_4$, and HCF_3SO_3 are 48, 48, and 52, as compared with $x = 17$ for a mostly second-stage $C_xC_8F_{17}SO_3$. This difference is primarily a consequence of the bilayer structure, where there are two anionic layers per gallery instead of one. As a first approximation, therefore, *x* might be expected to be half that for small-anion intercalation compounds.

A second reason for the different stoichiometries may lie in a change in the extent of solvent incorporation, which reduces repulsive interactions between inter-

(24) Molecular modelling calculations were done using Hyperchem software and an MM+ atomic force field set.

calated anions and accounts for much of the occupied volume in compounds with small anions. As an example, a typical formulation for graphite nitrate formed in nitric acid can be $C_xNO_3 \cdot 3HNO_3$, so that three-quarters of the intergallery volume is occupied by neutral species. The bilayer structure mediates the repulsive interactions between anionic centers with the favorable interaction between perfluorocarbon chains and may thereby reduce solvent incorporation. As a result of these effects, we have the unexpected result that these very large anions are about twice as abundant within the galleries (relative to graphitic carbon) than are smaller anions in other graphite compounds.

Molecular model simulations indicate that the anion layers should nestle significantly at the gallery centers to permit packing the bilayers into the observed gallery heights, which cannot be accomplished if the anions have a closely packed arrangement. One means of evaluating intercalant packing is to compare the "packing density" of the intercalant layer derived experimentally from the mass uptake and volume increase (1.5 g/cm^3 for the third-stage product) to those of related compounds. The density of liquid $C_8F_{17}SO_3H$ is ~1.9 g/cm^3, and that of crystalline Teflon is near 2.3. From these comparisons, it appears that the galleries in these evacuated products are relatively porous.

This model of large, relatively porous galleries obtained led to several other interesting questions. For instance, it may be that these compounds will exhibit chemistry similar to that of the organoclays. As a starting point, it should prove interesting to determine whether nonpolar molecules can be introduced into the hydrophobic region of the intercalated galleries.

Exfoliated or delaminated graphite is an important commercial material, used for applications such as high-temperature linings and gaskets. Aside from this consideration, the development of new methods for exfoliation, especially at ambient temperature, is important as a gateway into a new chemistry for graphite or graphene layers. Other workers have recently investigated a novel method to achieve exfoliation at ambient temperature using an electrolyte containing trifluoroacetic acid.[25] As described above, the HOPG chip and graphite powder electrodes utilized in our and previous studies[20] swell dramatically and then exfoliate during oxidation beyond the second-stage compound for $C_xC_8F_{17}SO_3$. Long reaction times are required to apply the >30 C/mmol of C required to exfoliate by direct anodization in $LiC_8F_{17}SO_3$(saturation)/CH_3NO_2, which proves inconvenient for the generation of useful quantities of the exfoliated material. As an alternative, the formation of mixed-anion compounds is investigated, where sulfate or perchlorate is initially incorporated at high rate into the galleries (anodization 1) and the perfluorooctanesulfonate is introduced subsequently (anodization 2). The idea is to co-intercalate the two anion types and find an appropriate ratio such that the expanded structure and consequent exfoliation occur during anodization 2. The first step is rapid (and can be performed even more rapidly by chemical methods), and if the small anions constitute the majority of incorporated species, the overall reaction sequence is considerably faster than in preparation of low-stage $C_xC_8F_{17}SO_3$.

Table 3. Coulometric and Gravimetric Data for Oxidation of (a) Graphite Sulfate or (b) Graphite Perchlorate in $LiC_8F_{17}SO_3$(saturated)/CH_3NO_2[a]

	in conc H_2SO_4			in $LiC_8F_{17}SO_3$(saturated)/CH_3NO_2	
	q1 (C/mmol of C)	$\Delta m1$ (mg/mmol of C)	*x1*	$\Delta m2$ (mg/mmol of C)	*x2*
a					
	0.48 (C_{200}^+)	2.1	4.7	7.1	93
	1.4 (C_{70}^+)	4.9	20	0.7	700
	2.2 (C_{44}^+)	6.6	14	−0.1	
b					
	1.4 (C_{70}^+)	4.9	21	4.1	120
	1.9 (C_{50}^+)	5.5	18	−0.1	
	2.4 (C_{41}^+)	7.9	13	−0.3	

[a] q1 is the charge applied to form graphite sulfate or perchlorate, $\Delta m1$ and $\Delta m2$ refer to mass changes measured following these oxidations. The mole ratios of carbon to intercalant, χ, are calculated from gravimetry as $C_xH_2SO_4$, C_xHClO_4, and $C_xC_8F_{17}SO_3$. The negative mass changes observed in some samples may reflect experimental error, although the slow decomposition of the graphene layers can occur at the potentials applied.

Initial results obtained are summarized in Table 3. The perfluoroanions are taken up only into the high-stage graphite sulfate or perchlorate compounds: at $x = 44$ (second stage) for sulfate and $x = 50$ for perchlorate no perfluoroanions are incorporated. These results can be understood by the presence of molecular acid that co-intercalates with the small anions. As prepared, the graphite sulfate and perchlorate contain a significant quantity of the neutral acid, for example, the formulation for the product following the first oxidation step in the first experiment would be approximately $C_{200}SO_4 \cdot mH_2SO_4$, where $m \approx (200/47) - 1 = 3.3$. These neutral molecules are not removed during the brief drying step, and can be converted to anionic form during anodization 2.[26] If a first-stage compound can be obtained by converting these neutral intercalants into anions, then no additional anions are incorporated by subsequent anodization. The most interesting behavior is observed during the second oxidation of $C_{70}SO_4 \cdot mH_2SO_4$, in which the compound exfoliates after the incorporation of only a relatively small amount of the perfluoranion. In this manner, ambient-temperature exfoliation may be realized much more rapidly than by direct formation of low-stage $C_xC_8F_{17}SO_3$. No exfoliation is observed during the anodization of perchlorate compound charged to a similar extent. SEM images of a pristine HOPG sample and the electrode following exfoliation of $C_{70}SO_4 \cdot mH_2SO_4$ in the $LiC_8F_{17}SO_3$(saturated)/CH_3NO_2 electrolyte (Figure 6) indicate that exfoliated product contains dissociated platelets approximately 1 μm thick, comparable in dimension to the thermally exfoliated graphites.[27]

Finally, an interesting observation is made during exfoliation of low-stage $C_xC_8F_{17}SO_3$ upon heating in an N_2 atmosphere. The accordian-like expansion of HOPG-based samples is partially reversible in that samples

(25) Bourelle, E.; Douglade, J.; Metrot, A. *Mol. Cryst. Liq. Cryst.* **1994**, *244*, 227.

(26) There remains some question over the identity and relative concentrations of intercalating species in the graphite sulfates (H_2SO_4, HSO_4^-, and/or SO_4^{2-}), and the second oxidation may involve either conversion of neutral to anionic form or HSO_4^- to SO_4^{2-}. In either case, the point remains that the product after the first anodization can be oxidized without taking up additional anions.

(27) Frackowiak, E.; Kaiser, W.; Krohn, H.; Beck, F. *Mol. Cryst. Liq. Cryst.* **1994**, *244*, 221.

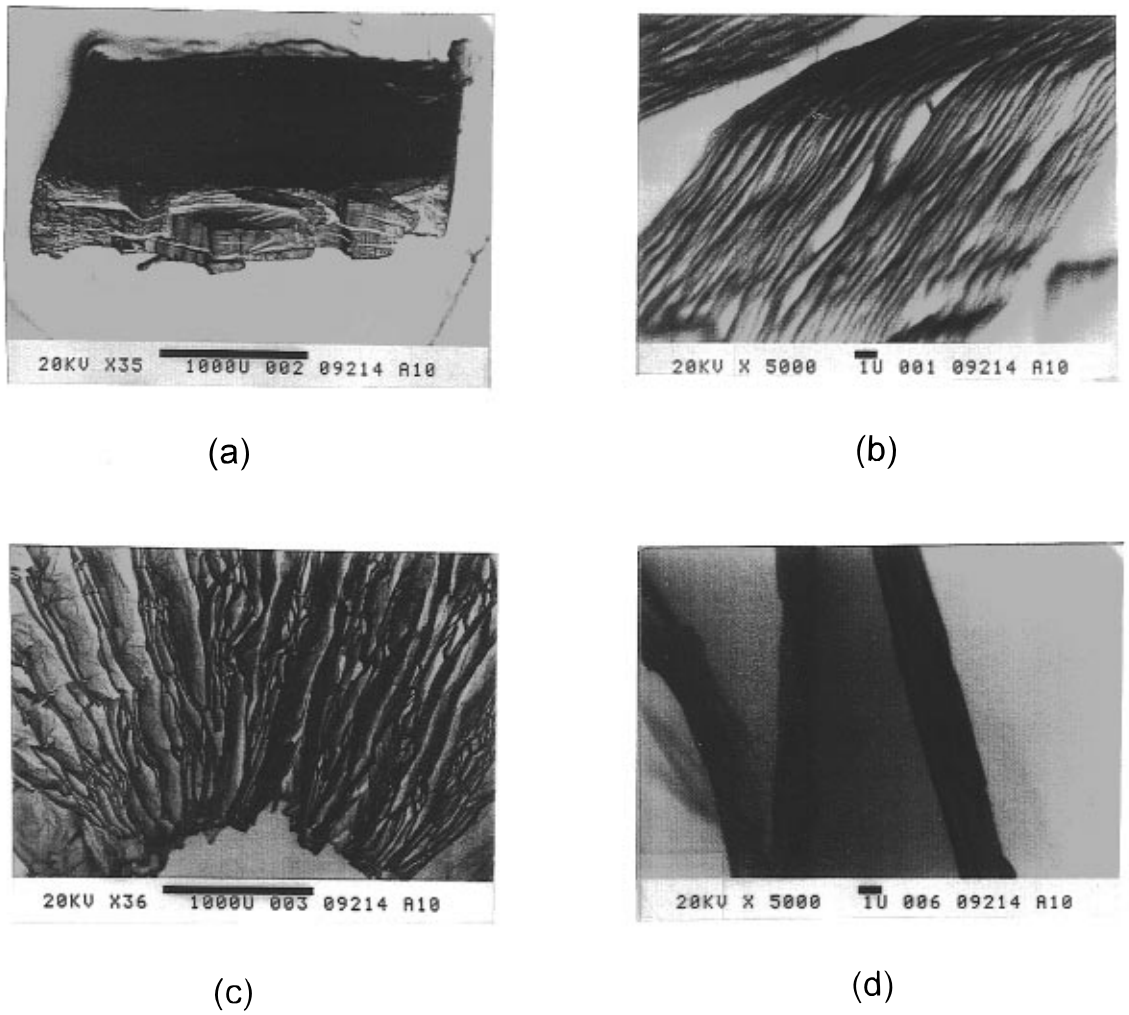

Figure 6. SEM images of (a, b) HOPG, and (c, d) HOPG delaminated at ambient temperature by oxidation of a graphite sulfate (C_{70}^{+}) in $LiC_8F_{17}SO_3$(saturated)/CH_3NO_2.

(original thickness = t_0) expand to $\sim 100t_0$ at approximately 200 °C and then collapse to $\sim 10t_0$ upon cooling to ambient temperature. The samples can undergo 20 or more alternations between $10t_0$ and $100t_0$ on temperature cycling. The graphite oxometallates, tested here under similar conditions, never undergo reversible expansion. XRD of the heated samples indicate the generation of both higher stage compounds and a graphitic material. The chemistry underlying this phenomenon has not been examined in detail; however, it seems likely the exfoliated platelets retain a surface coating of the perfluorooctanesulfonate surfactant and a hydrophobic cohesive interaction acts as a driving force for the reassembly of exfoliated platelets. The reversible expansion is not observed after heating in air, which is consistent with the displacement or decomposition of organoanions in the presence of water and O_2.

Acknowledgment. The authors gratefully acknowledge a supporting grant from the National Science Foundation (DMR-9157005).

CM950355V